Geophysical Journal International

Geophys. J. Int. (2018) **215,** 864–879
Advance Access publication 2018 July 31
GJI Gravity, geodesy and tides

doi: 10.1093/gji/ggy317

Recursive computation of gravitational field of a right rectangular parallelepiped with density varying vertically by following an arbitrary degree polynomial

Toshio Fukushima

National Astronomical Observatory/SOKENDAI, Ohsawa, Mitaka, Tokyo 181-8588, Japan. E-mail: Toshio.Fukushima@nao.ac.jp

Accepted 2018 July 28. Received 2018 July 26; in original form 2018 April 05

SUMMARY

We present a recursive formulation to compute the potential, the acceleration vector and the force gradient tensor of the gravitational field of a right rectangular parallelepiped or a prism when its volume mass density varies vertically by following an arbitrary degree polynomial. First, the potential of the parallelepiped is expressed as the triple difference of an indefinite volume integral. Next, for the density described by an arbitrary degree polynomial of the vertical coordinate, the integral is expressed as a finite sum of several elementary functions and three groups of auxiliary functions, the latter of which are recursively computable. Then, the acceleration vector and the force gradient tensor are obtained by analytically differentiating the potential. As a result, all the field quantities turn out to be linear combinations of seven basic functions: three arc tangents, three logarithms and a square root. Also, the employed recurrence formulae are as simple as of a leapfrog form. Thus, the execution of the new formulation is fast. For example, in the computation of the vertical gravity component only, it runs 30–2000 times faster than the existing formulation (Zhang & Jiang) when the maximum degree of polynomial increases from 2 to 40. However, the analytical expressions suffer from the catastrophic cancellation in the far region although they are accurate inside and near the prism.

Key words: Geopotential theory; Gravity anomalies and Earth structure; Magnetic anomalies: modelling and interpretation.

1 INTRODUCTION

Finding a precise and fast method to model the gravitational or geomagnetic field of a general object, such as the Earth and some major planets, the Moon and massive natural satellites, or heavy nearly spherical asteroids, is an important issue in geodesy, geophysics and planetary sciences (Heiskanen & Moritz 1967; Stacey & Davis 2008; de Pater & Lissauer 2010). The need of such a method is enlarged by the recent availability of dense topographic data such as obtained for the Earth by the Shuttle Radar Topography Mission (Smith & Sandwell 2003) and the Advanced Spacebourne Thermal Emission and Reflection Radiometer (Tachikawa *et al.* 2011). Indeed, both of them boast a fine spatial mesh size on the ground surface as small as 1 arcsec.

In principle, when the volume mass density distribution and the shape model of an object are provided, its gravitational quantities like the gravitational potential or the gravitational acceleration vector are expressed in terms of the Newton integrals (Laplace 1799). The same is also true for the magnetostatic field when the magnetic charge density distribution is known (Durand 1953). In fact, the investigation of the internal distribution of density or magnetic charge from the observed data of gravity and geomagnetism requires these forward model computation (Braitenberg *et al.* 2006; Sjöberg & Bagherbandi 2017). However, these integrals can be evaluated in a closed form only in special circumstances (Binney & Tremaine 2008). Well-known cases are spherically symmetric objects (Chandrasekhar 1995) and homogeneous ellipsoids (Chandrasekhar 1969). Other examples are found in the literature (Kellogg 1929; Lass 1950).

Thus, many researchers adopted an approach to decompose the given object into a sum of simple parts the gravitational or magnetostatic field of which is analytically integrable (Heck & Seitz 2007). Among such building blocks, a right rectangular parallelepiped or the so-called prism is mostly popular (Bessel 1813; Mollweide 1813). Other primitive objects preferred in geodesy are a polyhedron (Waldvogel 1979) and a tesseroid (Anderson 1976). Of course, the spherical tesseroid and its spheroidal extension are more suitable to model the field of nearly spherical or spheroidal objects like the Moon or the Earth. Nevertheless, the gravitational or magnetostatic field of the spherical tesseroid is

accurately determined only by a new type of the numerical integration (Fukushima 2018). The developed method is powerful and precise. Having stated so, we must admit that it is time-consuming.

In order to seek for a faster formulation, therefore, let us return to the decomposition methods using prism or polyhedrons (Wild-Pfeiffer 2008). Certainly, there are numerous works along this direction (D'Urso 2014; Conway 2015). Most of them assumed the homogeneity of the object for simplicity. Nonetheless, this is far from the reality (Jiang *et al.* 2017a). Thus, several studies tried to relax this restriction by assuming that the density varies by following a low-degree polynomial (D'Urso & Trotta 2017). Indeed, many density profiles are well approximated by a polynomial of the vertical coordinate (Rao 1985; Rao *et al.* 1990, 1995; Novak 2000; Eshagh 2009).

One may question about the usefulness of the prism model when the more versatile polyhedron formulation is available. However, the answer is still positive mainly because the computational complexity is much less and the CPU time is significantly smaller (Benedek *et al.* 2017). This preference has been enhanced by the availability of dense rectangular grid data (Smith & Sandwell 2003; Tachikawa *et al.* 2011). For example, the 20–30 m horizontal resolution on the Earth surface is so high that ignorable is the horizontal variation within the prism not only of the density but also of the heights of top and/or bottom surfaces. Also, most of the curvature effects in the regional model may be absorbed by adopting a global rectangular coordinate system and conducting the corresponding transformation of the topographic data.

On the other hand, rather large is the vertical size of the prisms to be considered in the terrain field modelling, say 10 km or so. This is the main reason why focused has been the effect of the vertical density contrast on the classic field of the prism (Rao 1985). For instance, the analytical formulae of the prismatic gravitational field have been obtained when its density is varying linearly (Garcia-Abdeslem 1992), quadratically (Rao *et al.* 1990) and cubically (Garcia-Abdeslem 2005). Similar formulae for general polyhedra are available up to the third-order polynomials (D'Urso & Trotta 2017).

Nevertheless, the observed vertical density profiles are more complicated (Li 2001). Indeed, some of them are well approximated by an exponential function (Cordell 1973; Granser 1987; Chai & Hinze 1988; Sjöberg & Nahavandchi 2000; Chappell & Kusznir 2008; Eshagh 2009; Eshagh & Sjöberg 2009; Karcol 2011; Chakravarthi *et al.* 2013) or a rational function (Rao *et al.* 1995; Sjöberg 1998; Chakravarthi *et al.* 2002). Figs 2 and 3 of Jiang *et al.* (2017a) illustrate clear examples where seventh- or eighth-order polynomials are needed to fit the observed density profiles. In such cases, high-degree polynomials are demanded to model the vertical inhomogeneity precisely.

Recently, Zhang & Jiang (2017) presented the analytical formulae of the three rectangular components of the gravitational acceleration vector for a prism with the density varying as an arbitrary degree polynomial. Also, Jiang *et al.* (2017b) added the similar formulae for the six rectangular components of the gravity gradient tensor. Both of these expressions consist of, apart from a few terms of elementary functions, the double series of the rectangular coordinates and a square root of their squared sum. Consequently, the actual computation procedure is so complicated that the achieved computational accuracy is as low as five digits or less. Also, they do not provide the formula of the gravitational potential itself, which is important in the geoid determination.

Therefore, in order to extend the solution coverage of the prismatic gravitational field to the potential, we developed a systematic formulation to compute not only the potential but also the gravity vector and its gradient tensor by employing some recurrence formulae. As a result, both the computational precision and the computational speed are significantly improved as will be shown later.

Below, we explain the new formulation in Section 2, and describe the results of its numerical experiments in Section 3. Also, Appendices provide the detailed derivation of the recursive formulation to compute the gravitational potential and its partial derivatives.

2 METHOD

2.1 Analytical computation of gravitational potential of vertically inhomogeneous prism

Let us denote by (x, y, z) the rectangular coordinates of an evaluation point in the 3-D space and by (x', y', z') those of a mass element inside a prism, namely a right rectangular parallelepiped. To be more specific, we define the geometric domain of the prism as

$$x_1 \le x' \le x_2, \quad y_1 \le y' \le y_2, \quad z_1 \le z' \le z_2. \tag{1}$$

Then, the negative gravitational potential of the prism at the evaluation point is expressed by a definite volume integral as

$$V(x, y, z) \equiv G \int_{z_1}^{z_2} \int_{y_1}^{y_2} \int_{x_1}^{x_2} \frac{\rho\,(x', y', z')\,\mathrm{d}x'\mathrm{d}y'\mathrm{d}z'}{\sqrt{(x'-x)^2 + (y'-y)^2 + (z'-z)^2}}, \tag{2}$$

where G is Newton's constant of universal attraction and $\rho(x', y', z')$ is the volume mass density of the prism.

Assume that the density within the prism is described by a polynomial of the vertical coordinate as

$$\rho\left(x', y', z'\right) = \sum_{n=0}^{N} \left[\rho_n \cdot \left(z'\right)^n\right]. \tag{3}$$

Then, the resulting gravitational potential is similarly expanded as

$$V(x, y, z) = \sum_{n=0}^{N} V_n(x, y, z), \tag{4}$$

where $V_n(x, y, z)$ is defined as

$$V_n(x, y, z) \equiv G\rho_n \int_{z_1}^{z_2} (z')^n \left(\int_{y_1}^{y_2} \int_{x_1}^{x_2} \frac{\mathrm{d}x'\mathrm{d}y'}{\sqrt{(x'-x)^2 + (y'-y)^2 + (z'-z)^2}} \right) \mathrm{d}z'. \tag{5}$$

By changing the integration variables from x', y', and z' to X, Y and Z defined as

$$X \equiv x' - x, \quad Y \equiv y' - y, \quad Z \equiv z' - z, \tag{6}$$

and expanding $(z')^n$ into a polynomial of Z as

$$(z')^n = (Z + z)^n = \sum_{m=0}^{n} \binom{n}{m} Z^m z^{n-m}, \tag{7}$$

we rewrite $V_n(x, y, z)$ formally into a degree n polynomial of z as

$$V_n(x, y, z) = G\rho_n \sum_{m=0}^{n} \binom{n}{m} W_m(x, y, z) z^{n-m}, \tag{8}$$

where $W_m(x, y, z)$ is a weight function expressed as a definite volume integral and rewritten as a triple difference of an indefinite volume integral as

$$W_m(x, y, z) \equiv \int_{Z_1}^{Z_2} Z^m \left(\int_{Y_1}^{Y_2} \int_{X_1}^{X_2} \frac{\mathrm{d}X\mathrm{d}Y}{\sqrt{X^2 + Y^2 + Z^2}} \right) \mathrm{d}Z = \Delta_3 U_m, \tag{9}$$

where X_i, Y_j and Z_k are the shifted endpoints defined as

$$X_i \equiv x_i - x, \quad Y_j \equiv y_j - y, \quad Z_k \equiv z_k - z, \tag{10}$$

Δ_3 is the triple difference operator defined for an arbitrary function $f(X, Y, Z)$ as

$$\begin{aligned} \Delta_3 f \equiv\ & f(X, Y, Z)\Big|_{Z=Z_1}^{Z=Z_2}\Big|_{Y=Y_1}^{Y=Y_2}\Big|_{X=X_1}^{X=X_2} = \sum_{i=1}^{2}\sum_{j=1}^{2}\sum_{k=1}^{2}(-1)^{i+j+k} f\left(X_i, Y_j, Z_k\right) \\ =\ & f(X_2, Y_2, Z_2) - f(X_2, Y_2, Z_1) - f(X_2, Y_1, Z_2) + f(X_2, Y_1, Z_1) \\ & - f(X_1, Y_2, Z_2) + f(X_1, Y_2, Z_1) + f(X_1, Y_1, Z_2) - f(X_1, Y_1, Z_1), \end{aligned} \tag{11}$$

and $U_m(X, Y, Z)$ is an indefinite volume integral defined as

$$U_m(X, Y, Z) \equiv \int^{Z} Z^m \left(\int^{Y} \int^{X} \frac{\mathrm{d}X\mathrm{d}Y}{\sqrt{X^2 + Y^2 + Z^2}} \right) \mathrm{d}Z, \tag{12}$$

which we name the potential function of degree m.

By substituting the rewritten expression of $V_n(x, y, z)$, eq. (8), into the summation form of $V(x, y, z)$, eq. (4), we obtain its further rewriting in terms of $W_m(x, y, z)$ as

$$\begin{aligned} V(x, y, z) &= \sum_{n=0}^{N} \left[G\rho_n \sum_{m=0}^{n} \binom{n}{m} W_m(x, y, z) z^{n-m} \right] = \sum_{m=0}^{N}\sum_{n=m}^{N} G\rho_n \binom{n}{m} W_m(x, y, z) z^{n-m} \\ &= \sum_{m=0}^{N} \left[\sum_{j=0}^{N-m} G\rho_{j+m} \binom{j+m}{m} z^j \right] W_m(x, y, z) = \sum_{m=0}^{N} c_m(z) W_m(x, y, z), \end{aligned} \tag{13}$$

where j is the dummy index defined as $j \equiv n - m$ and $c_m(z)$ is the mth coefficient polynomial expressed as

$$c_m(z) \equiv \sum_{j=0}^{N-m} c_{mj} z^j, \tag{14}$$

and c_{mj} is its jth coefficient defined as

$$c_{mj} \equiv \binom{j+m}{m} G\rho_{j+m}. \tag{15}$$

Since c_{mj} is calculated from ρ_n, which is already specified, and $W_m(x, y, z)$ can be computed from $U_m(X, Y, Z)$, now the problem is reduced to the evaluation of the potential function, $U_m(X, Y, Z)$.

2.2 Analytical computation of acceleration vector and force gradient tensor

Once the analytical expression of the potential is given, the associated acceleration vector and force gradient tensor are mechanically derived by its first- and second-order partial differentiation, respectively (Kellogg 1929; Lass 1950; Durand 1953). Thus, the rectangular components of the gravitational acceleration vector, $g_x(x, y, z)$, $g_y(x, y, z)$ and $g_z(x, y, z)$, are explicitly given as

$$g_x(x,y,z) = \sum_{n=0}^{N} c_n(z)\left(\frac{\partial W_n}{\partial x}\right), \quad g_y(x,y,z) = \sum_{n=0}^{N} c_n(z)\left(\frac{\partial W_n}{\partial y}\right),$$
$$g_z(x,y,z) = \sum_{n=0}^{N}\left[c_n(z)\left(\frac{\partial W_n}{\partial z}\right) + c_n'(z)W_n\right]. \tag{16}$$

Also, those of the gravity gradient tensor, $\Gamma_{xx}(x, y, z)$ through $\Gamma_{zz}(x, y, z)$, are computed as

$$\Gamma_{xx}(x,y,z) = \sum_{n=0}^{N} c_n(z)\left(\frac{\partial^2 W_n}{\partial x\partial x}\right), \quad \Gamma_{xy}(x,y,z) = \sum_{n=0}^{N} c_n(z)\left(\frac{\partial^2 W_n}{\partial x\partial y}\right),$$
$$\Gamma_{yy}(x,y,z) = \sum_{n=0}^{N} c_n(z)\left(\frac{\partial^2 W_n}{\partial y\partial y}\right), \quad \Gamma_{xz}(x,y,z) = \sum_{n=0}^{N}\left[c_n(z)\left(\frac{\partial^2 W_n}{\partial x\partial z}\right) + c_n'(z)\left(\frac{\partial W_n}{\partial x}\right)\right],$$
$$\Gamma_{yz}(x,y,z) = \sum_{n=0}^{N}\left[c_n(z)\left(\frac{\partial^2 W_n}{\partial y\partial z}\right) + c_n'(z)\left(\frac{\partial W_n}{\partial y}\right)\right],$$
$$\Gamma_{zz}(x,y,z) = \sum_{n=0}^{N}\left[c_n(z)\left(\frac{\partial^2 W_n}{\partial z\partial z}\right) + 2c_n'(z)\left(\frac{\partial W_n}{\partial z}\right) + c_n''(z)W_n\right]. \tag{17}$$

In the above, $c_n'(z)$ and $c_n''(z)$ are the first- and second-order derivatives of $c_n(z)$ with respect to z expressed as

$$c_n'(z) \equiv \frac{dc_n}{dz} = \sum_{m=0}^{N-n-1} c_{nm}' z^m, \quad c_n''(z) \equiv \frac{d^2 c_n}{dz^2} = \sum_{m=0}^{N-n-2} c_{nm}'' z^m, \tag{18}$$

where c_{nm}' and c_{nm}'' are their coefficients written as

$$c_{nm}' \equiv (m+1)\binom{n+m+1}{n} G\rho_{n+m+1}, \quad c_{nm}'' \equiv (m+2)(m+1)\binom{n+m+2}{n} G\rho_{n+m+2}. \tag{19}$$

Also, the first- and second-order partial derivatives of $W_n(x, y, z)$ are expressed as triple differences of the corresponding partial derivatives of $U_n(X, Y, Z)$ as

$$\frac{\partial W_n}{\partial x} = -\Delta_3 U_{nX}, \quad \frac{\partial W_n}{\partial y} = -\Delta_3 U_{nY}, \quad \frac{\partial W_n}{\partial z} = -\Delta_3 U_{nZ}, \quad \frac{\partial^2 W_n}{\partial x\partial x} = \Delta_3 U_{nXX}, \quad \frac{\partial^2 W_n}{\partial x\partial y} = \Delta_3 U_{nXY},$$
$$\frac{\partial^2 W_n}{\partial x\partial z} = \Delta_3 U_{nXZ}, \quad \frac{\partial^2 W_n}{\partial y\partial y} = \Delta_3 U_{nYY}, \quad \frac{\partial^2 W_n}{\partial y\partial z} = \Delta_3 U_{nYZ}, \quad \frac{\partial^2 W_n}{\partial z\partial z} = \Delta_3 U_{nZZ}, \tag{20}$$

where $U_{nX}(X, Y, Z)$ through $U_{nZZ}(X, Y, Z)$ are the partial derivatives of $U_n(X, Y, Z)$ defined as

$$U_{nX}(X,Y,Z) \equiv \frac{\partial U_n}{\partial X}, \quad U_{nY}(X,Y,Z) \equiv \frac{\partial U_n}{\partial Y}, \quad U_{nZ}(X,Y,Z) \equiv \frac{\partial U_n}{\partial Z},$$
$$U_{nXX}(X,Y,Z) \equiv \frac{\partial^2 U_n}{\partial X\partial X}, \quad U_{nXY}(X,Y,Z) \equiv \frac{\partial^2 U_n}{\partial X\partial Y}, \quad U_{nXZ}(X,Y,Z) \equiv \frac{\partial^2 U_n}{\partial X\partial Z},$$
$$U_{nYY}(X,Y,Z) \equiv \frac{\partial^2 U_n}{\partial Y\partial Y}, \quad U_{nYZ}(X,Y,Z) \equiv \frac{\partial^2 U_n}{\partial Y\partial Z}, \quad U_{nZZ}(X,Y,Z) \equiv \frac{\partial^2 U_n}{\partial Z\partial Z}. \tag{21}$$

Note the sign change in the first-order derivatives caused by the differential relation of the coordinates as

$$\mathrm{d}X = -\mathrm{d}x, \quad \mathrm{d}Y = -\mathrm{d}y, \quad \mathrm{d}Z = -\mathrm{d}z. \tag{22}$$

In any case, the problem is reduced to the computation of the partial derivatives of the potential functions.

2.3 Special case: homogeneous prism

Before going further, we quote the well-known result when $n = 0$, namely of the homogeneous prism (MacMillan 1930, section 43). Hereafter, we omit the argument dependence of the potential functions and their partial derivatives as well as other functions on X, Y and Z for simplicity.

Then, we express the formulae compactly as

$$\begin{aligned} U_0 &= -\left(X^2A + Y^2B + Z^2C\right)/2 + YZD + ZXE + XYF, \\ U_{0X} &= -XA + YF + ZE, \quad U_{0Y} = XF - YB + ZD, \quad U_{0Z} = XE + YD - ZC, \\ U_{0XX} &= -A, \quad U_{0XY} = F, \quad U_{0XZ} = E, \quad U_{0YY} = -B, \quad U_{0YZ} = D, \quad U_{0ZZ} = -C, \end{aligned} \tag{23}$$

where A through F are elementary functions defined as

$$\begin{aligned} &A \equiv \tan^{-1}\left(\frac{YZ}{XR}\right), \quad B \equiv \tan^{-1}\left(\frac{ZX}{YR}\right), \quad C \equiv \tan^{-1}\left(\frac{XY}{ZR}\right), \\ &D \equiv \ln(X+R), \quad E \equiv \ln(Y+R), \quad F \equiv \ln(Z+R), \end{aligned} \tag{24}$$

and R stands for

$$R \equiv \sqrt{X^2 + Y^2 + Z^2}. \tag{25}$$

2.4 Recursive computation of potential functions

Let us consider an efficient way to compute U_n and its partial derivatives, U_{nX} through U_{nZZ}, for a group of positive indices, $n = 1, 2, \ldots,$ and N. We begin with U_n. As explained in Appendix A, its analytical expression is derived as

$$U_n = -\frac{Z^{n+2}C}{n+2} + \frac{Z^{n+1}(YD + XE)}{n+1} - \frac{YD_{n+2} + XE_{n+2}}{(n+1)(n+2)}. \tag{26}$$

Here, D_n and E_n are the quantities computed recursively as

$$D_n = -Y^2 D_{n-2} - XR_{n-2}, \quad E_n = -X^2 E_{n-2} - YR_{n-2}, \tag{27}$$

from their starting values prepared as

$$D_1 = D, \quad D_2 = YB - XF, \quad E_1 = E, \quad E_2 = XA - YF. \tag{28}$$

Also, R_n are additional quantities computed recursively as

$$R_n = \left[Z^{n-1}R - (n-1)SR_{n-2}\right]/n, \tag{29}$$

with the initial values computed as

$$R_1 = R, \quad R_2 = (ZR - SF)/2, \tag{30}$$

where S is the squared sum of the horizontal coordinates written as

$$S \equiv X^2 + Y^2. \tag{31}$$

By using the Mathematica (Wolfram 2003), we confirmed the correctness of eq. (26) by examining its differential definition:

$$\frac{\partial^3 U_n}{\partial X \partial Y \partial Z} = \frac{Z^n}{R}. \tag{32}$$

We omit the details of the lateral validation for saving the space. At any rate, this recursive procedure to compute U_n is entirely new.

2.5 Analytical computation of derivatives of U_n

Let us move on to the partial derivatives of U_n for a positive integer n. As explained in Appendix B, they are explicitly computed from the quantities introduced in the previous subsections as

$$\begin{aligned} U_{nX} &= \frac{Z^{n+1}E - E_{n+2}}{n+1}, \quad U_{nY} = \frac{Z^{n+1}D - D_{n+2}}{n+1}, \quad U_{nZ} = -Z^{n+1}C + Z^n(YD + XE), \\ U_{nXX} &= XE_n, \quad U_{nXY} = R_n, \quad U_{nXZ} = Z^n E, \quad U_{nYY} = YD_n, \quad U_{nYZ} = Z^n D, \\ U_{nZZ} &= -(n+1)Z^n C + nZ^{n-1}(YD + XE). \end{aligned} \tag{33}$$

By means of the Mathematica again, these expressions can be easily validated by examining their differential definitions:

$$\frac{\partial^3 U_{nX}}{\partial X\partial Y\partial Z}=\frac{-XZ^n}{R^3},\quad \frac{\partial^3 U_{nY}}{\partial X\partial Y\partial Z}=\frac{-YZ^n}{R^3},\quad \frac{\partial^3 U_{nZ}}{\partial X\partial Y\partial Z}=\frac{\left[nS+(n-1)Z^2\right]Z^{n-1}}{R^3},$$
$$\frac{\partial^3 U_{nXX}}{\partial X\partial Y\partial Z}=\frac{\left(2X^2-Y^2-Z^2\right)Z^n}{R^5},\quad \frac{\partial^3 U_{nXY}}{\partial X\partial Y\partial Z}=\frac{3XYZ^n}{R^5},\quad \frac{\partial^3 U_{nXZ}}{\partial X\partial Y\partial Z}=\frac{-\left[nS+(n-3)Z^2\right]XZ^{n-1}}{R^5},$$
$$\frac{\partial^3 U_{nYY}}{\partial X\partial Y\partial Z}=\frac{\left(-X^2+2Y^2-Z^2\right)Z^n}{R^5},\quad \frac{\partial^3 U_{nYZ}}{\partial X\partial Y\partial Z}=\frac{-\left[nS+(n-3)Z^2\right]YZ^{n-1}}{R^5},$$
$$\frac{\partial^3 U_{nZZ}}{\partial X\partial Y\partial Z}=\frac{Z^{n-2}}{R^5}\left[n(n-1)S^2+\left(2n^2-4n-1\right)SZ^2+(n-2)(n-1)Z^4\right]. \tag{34}$$

It is noteworthy that no new functions are needed in the derivative computation, since all of A through F as well as D_n, E_n, and R_n have already appeared in the procedure to compute U_n as described in the previous subsection. Also, the derivative formulae, eq. (33), are compact. As a result, their evaluation can be executed very efficiently, namely with a small amount of additional computational labour.

These expressions of the acceleration vector components and the gravity gradient tensor components are, apart from the reducible contributions, equivalent with the previous results (Zhang & Jiang 2017; Jiang *et al.* 2017b). Indeed, the special function, $\varphi_j(x, z)$, introduced in eq. (18) of Zhang & Jiang (2017) is, except for the reducible contributions, mathematically equivalent with D_n and E_n in the sense

$$D_n=-X\varphi_{n-1}(Y,Z),\quad E_n=-Y\varphi_{n-1}(X,Z). \tag{35}$$

Refer to eq. (A9) showing the equivalence in Appendix A.

In any case, the explicit expressions of $\varphi_j(x, z)$ provided in eqs (24) and (30) of Zhang & Jiang (2017) contain a triple series of the relative coordinates and the mutual distance. Therefore, its numerical evaluation is time-consuming when j is high. In this sense, the recursive formulation presented here is much better in the viewpoint of the computational speed.

2.6 Hints for robust numerical evaluation

Before closing the explanation of the new method, we make a remark on the singularities of V and its partial derivatives. The procedures described in the previous subsections guarantee that the final explicit expressions of U_n through U_{nZZ} are weighted linear sums of A through F and R with the coefficients written as polynomials of X, Y and Z.

Consequently, the non-analytic feature of V and its partial derivatives are only those inherited from the seven basic functions, A through F and R. In other words, the issue of the singularity on the analytical expressions of the gravitational field of a vertically inhomogeneous prism is the same as that of the homogeneous prism (Nagy *et al.* 2000; Tsoulis & Petrovic 2001).

In the actual numerical evaluation of U_n through U_{nZZ}, we compute A through F and R as

$$\begin{aligned}&A=atan3(X,Y,Z),\quad B=atan3(Y,Z,X),\quad C=atan3(Z,X,Y),\\&D=logsum(X,Y,Z),\quad E=logsum(Y,Z,X),\quad F=logsum(Z,X,Y),\\&R=\sqrt{X^2+Y^2+Z^2+\omega},\end{aligned} \tag{36}$$

where $atan3(\xi,\eta,\zeta)$ and $logsum(\xi,\eta,\zeta)$ are special functions defined conditionally as

$$atan3(\xi,\eta,\zeta)\equiv\begin{cases}\tan^{-1}\left(\frac{\eta\zeta}{\xi\sqrt{\xi^2+\eta^2+\zeta^2}}\right), & (\xi\neq 0),\\ 0, & (\xi=0),\end{cases} \tag{37}$$

$$logsum(\xi,\eta,\zeta)\equiv\begin{cases}\ln\left(\xi+\sqrt{\xi^2+\eta^2+\zeta^2}\right), & (\xi>0),\\ (1/2)\ln\left(\eta^2+\zeta^2+\omega\right), & (\xi=0),\\ \ln\left(\frac{\eta^2+\zeta^2+\omega}{\sqrt{\xi^2+\eta^2+\zeta^2}-\xi}\right), & (\xi<0),\end{cases} \tag{38}$$

and ω is a tiny positive constant defined as

$$\omega\equiv 10^{-150}. \tag{39}$$

The introduction of the switch structure in the *logsum* function is mainly so as to suppress the information loss in the argument computation of the logarithm. The other modifications are in order to avoid the computational troubles caused by the non-numerical values such as $Infinity$ or NaN (IEEE 2008). These answers are undesirable since they ruin the following computations. They are returned mainly because of the zero divisions, which may happen on the surfaces of, along the edges of, and/or at the vertices of the prism (Nagy *et al.* 2000). This does not happen *if* the above modifications are introduced. Anyhow, the introduction of this recipe is effective to treat these practical problems properly without degrading the computational accuracy significantly.

3 NUMERICAL EXPERIMENTS

3.1 Computational error

The correctness of the new formulation is analytically confirmed in Appendices A and B. Also, the lateral examination of the differential definitions of U_n through U_{nZZ} validate their formulae. Therefore, let us focus on the numerical errors which will be faced when using the new formulation. For this purpose, we check the self-consistency of the analytically computed gravitational field. More closely speaking, we evaluate $\rho_G(x, y, z)$, the density recovered from $\Gamma_{xx}(x, y, z)$, $\Gamma_{yy}(x, y, z)$ and $\Gamma_{zz}(x, y, z)$, the diagonal components of the computed gravity gradient tensor. Mathematically, the recovered density is defined as

$$\rho_G(x, y, z) \equiv -\left(\frac{\Gamma_{xx}(x, y, z) + \Gamma_{yy}(x, y, z) + \Gamma_{zz}(x, y, z)}{4\pi G}\right). \tag{40}$$

This is nothing but a rewriting of Poisson's equation. Next, we measure its error as

$$\delta\rho(x, y, z) \equiv \frac{\rho_G(x, y, z) - \rho_M(x, y, z)}{\max\rho}, \tag{41}$$

where $\max\rho$ is the maximum value of $\rho(x, y, z)$. Here, the reference value, $\rho_M(x, y, z)$, is a local mean value of $\rho(x, y, z)$ defined as

$$\rho_M(x, y, z) \equiv \lim_{r\to 0}\left(\frac{3}{4\pi r^3}\int_{x^2+y^2+z^2\le r^2}\rho(x, y, z)\mathrm{d}x\,\mathrm{d}y\mathrm{d}z\right). \tag{42}$$

Namely, it is a limit value of the average of the density over a small sphere centered at the evaluation point. Note that this quantity is well defined even when the original density $\rho(x, y, z)$ has a finite discontinuity, and therefore indeterminate. In the case of prisms, the discontinuities occur at the vertices, along the edges, or on the surfaces of the prism. As a result, if a prism is appropriately rotated such that its edges are in parallel to the coordinate axes, the integral expression is compactly rewritten as

$$\begin{aligned}\rho_M(x, y, z) = \frac{1}{8}\lim_{\xi\to 0+0}\lim_{\eta\to 0+0}\lim_{\zeta\to 0+0}[&\rho(x+\xi, y+\eta, z+\zeta) + \rho(x-\xi, y+\eta, z+\zeta)\\ &+\rho(x+\xi, y-\eta, z+\zeta) + \rho(x-\xi, y-\eta, z+\zeta) + \rho(x+\xi, y+\eta, z-\zeta)\\ &+\rho(x-\xi, y+\eta, z-\zeta) + \rho(x+\xi, y-\eta, z-\zeta) + \rho(x-\xi, y-\eta, z-\zeta)].\end{aligned} \tag{43}$$

For example, if the prism is homogeneous and its non-zero density value is ρ_0, the modified density function is explicitly written as

$$\rho_M(x, y, z) = \begin{cases}\rho_0/8, & \text{(if at the vertices of the prism),}\\ \rho_0/4, & \text{(else if along the edges of the prism),}\\ \rho_0/2, & \text{(else if on the surfaces of the prism),}\\ \rho_0, & \text{(else if inside the prism),}\\ 0, & \text{(otherwise).}\end{cases} \tag{44}$$

At any rate, the density recovery error should be zero since Poisson's equation must hold everywhere. In other words, its deviation from the zero value indicates a sort of accumulated round-off errors during the actual execution of the new formulation.

As a simple example, let us examine the computational error of a unit cubic prism occupying the 3-D domain,

$$0 \le x \le 1, 0 \le y \le 1, \text{ and } 0 \le z \le 1. \tag{45}$$

Assume that the prism is inhomogeneous in the sense such that ρ is a degree n monomial of z as

$$\rho(z) = \rho_0 z^n, \tag{46}$$

for some values of n as $n = 0$, 1,..., and 10. Thus, the maximum density value becomes $\max\rho = \rho_0$. For this prism, Fig. 1 illustrates $\delta\rho$ obtained by the new formulation in the quadruple precision environment. The evaluation is done inside and above the prism in a wide range as $10^{-3} \le z \le 10^{15}$, and along a vertical straight line passing through the prism where the x- and y-coordinates of the evaluation point are fixed as non-trivial values as $x = 1/4$ and $y = 3/5$. The errors are displayed as a function of the vertical coordinate in a log–log manner. Evidently, the errors remain at the level of the quadruple precision machine epsilon, $\epsilon_Q \equiv 2^{-113} \approx 9.63 \times 10^{-35}$, when the distance from the coordinate origin, namely $|z|$ in this specific case, is sufficiently small and/or $n = 0$. Otherwise, they dramatically grow when the distance increases. Without doubt, this error growth is due to the round-off errors in a certain process in the new formulation to compute Γ_{xx}, Γ_{yy} and/or Γ_{zz} because the correctness of their expressions is analytically confirmed.

Next, as a practical example, we prepared Fig. 2 showing the density recovery error of a vertically inhomogeneous prism with an exponentially damped density profile (Cordell 1973; Granser 1987; Chai & Hinze 1988; Chappell & Kusznir 2008; Eshagh & Sjöberg 2009; Karcol 2011; Chakravarthi *et al.* 2013). Again, the prism was chosen as a unit cube occupying the 3-D volume defined as $0 \le x \le 1$, $0 \le y \le 1$ and $0 \le z \le 1$. Meanwhile, the density profile was set as a polynomial obtained by truncating the Maclaurin series of an exponential function as

$$\rho(z) \equiv \rho_0\sum_{n=0}^{N}\frac{(-z)^n}{n!} \approx \rho_0\exp(-z), \tag{47}$$

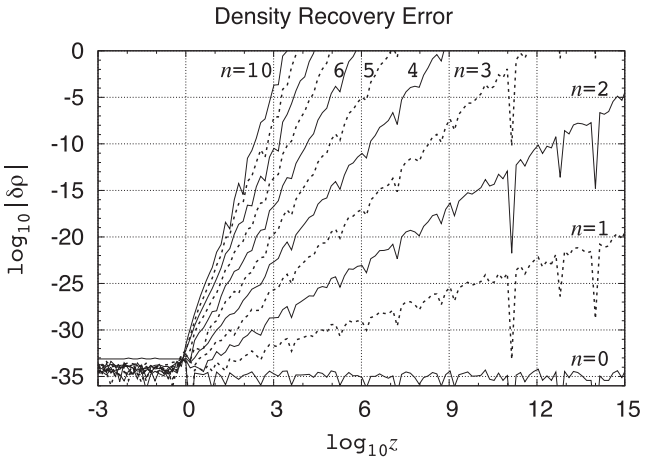

Figure 1. Density recovery error of prismatic gravitational field. Illustrated are $\delta\rho$, the scaled density recovery errors of the gravitational field of an inhomogeneous prism. The errors are measured as $\delta\rho(x, y, z) \equiv -[\{\Gamma_{xx}(x, y, z) + \Gamma_{yy}(x, y, z) + \Gamma_{zz}(x, y, z)\}/(4\pi G) + \rho_M(x, y, z)]/\rho_0$, where Γ is the gravity gradient tensor, $\rho_M(x, y, z)$ is the modified density function defined in the main text and ρ_0 is a nominal constant. We assume that the density of the prism follows a degree n monomial of z. The errors are plotted as a function of z in a log–log manner for a wide range of z as $10^{-3} \leq z \leq 10^{15}$. Here, x and y are fixed as non-trivial values as $x = 1/4$ and $y = 3/5$, respectively. The curves show the results for several values of n as $n = 0, 1, ..., 10$. They are drawn by solid lines for even degrees are by broken lines otherwise. Evidently, the errors remain almost constant within the prism but increase in proportion to z^n outside.

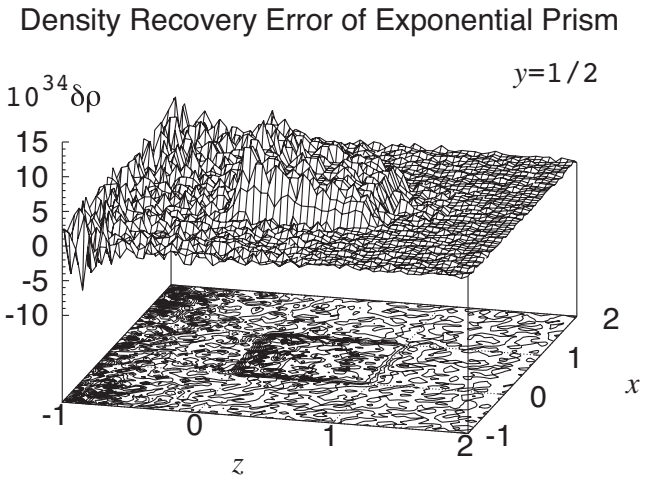

Figure 2. Bird's-eye view of density recovery error of exponentially damped prism: x–z plane, y=1/2. Presented are the bird's-eye view and the associated contour map of $\delta\rho(x, y, z)$, the density recovery error, of a vertically inhomogeneous prism with an exponentially damped density profile obtained in the quadruple precision computation. The errors are displayed as a function of x and z in the domain $-1 \leq x \leq 2$ and $-1 \leq z \leq 2$, while the y-coordinate is fixed as $y = 1/2$. The displayed domain well covers that of the prism, $0 \leq x \leq 1$, $0 \leq y \leq 1$ and $0 \leq z \leq 1$.

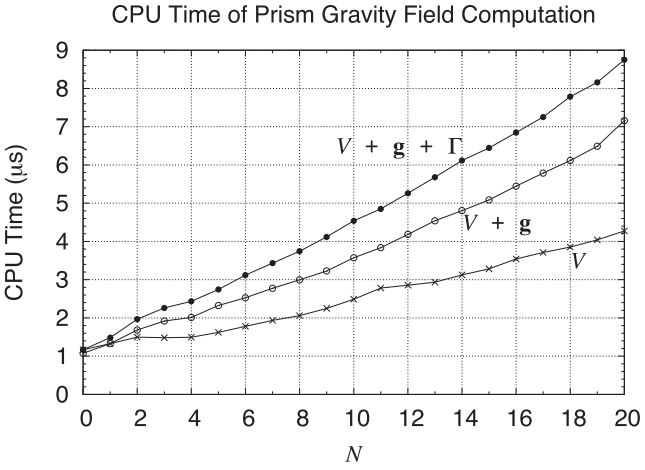

Figure 3. Averaged CPU time of gravity field computation. Shown are the averaged CPU time required to compute the gravitational quantities of a prism by the new formulation as a function of N, the maximum degree of the vertical density polynomial. The CPU time was measured at a consumer PC with the Intel Core i7-4600 U CPU running at 2.10 GHz clock. Compared are the three cases: (i) the computation of V only, (ii) the computation of V, g_x, g_y and g_z simultaneously and (iii) the computation of the full set of V, g_x, g_y, g_z and Γ_{xx} through Γ_{zz}. We experimentally find that 24 ns is the averaged CPU time at the same PC for one execution of the elementary functions like the natural logarithm or the arc tangent function.

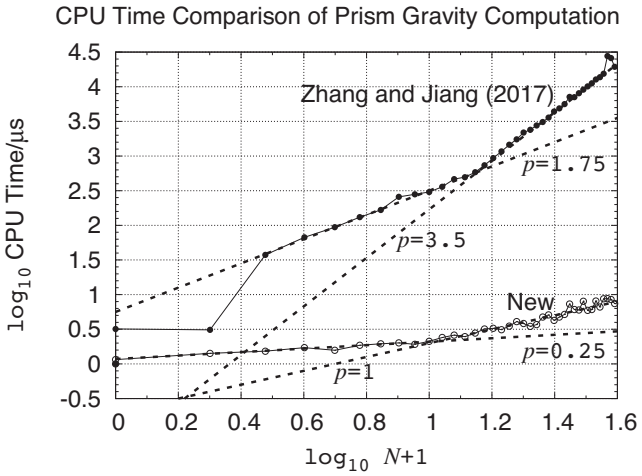

Figure 4. Comparison of CPU time of vertical gravity computation. Same as Fig. 3, but compared are the CPU times to compute g_z by (i) the existing method (Zhang & Jiang 2017), and (ii) the new method. This time, the results of the cases $0 \le N \le 40$ are plotted in a log–log manner with respect to the number of monomial terms, $N + 1$. The broken lines indicate piecewise power-law curves fit to the measurements where p indicates the estimated power-law index.

where $N = 18$ and 31 in the double and quadruple precision computation, respectively. The relative approximation errors of this truncated series are less than the corresponding machine epsilon in the region $0 \le z \le 1$, since $1/(19!) \approx 8.22 \times 10^{-18} < \epsilon_D$ and $1/(32!) \approx 3.80 \times 10^{-36} < \epsilon_Q$. As a result, there remains no practical difference between the usage of the polynomial approximation and the direct computation of the exponential function. At any rate, Fig. 2 illustrates $\delta\rho$ for this exponentially damped prism obtained by the quadruple precision computation of the new formulation. Again, the errors are sufficiently small.

3.2 Computational time

Let us move to the aspect of the computational time. More concretely speaking, we measured the CPU time to prepare a number of the numerical values of the gravitational field of an inhomogeneous prism by using the new formulation. Actually, we evaluated 10 millions of V, g_x, g_y, g_z and/or Γ_{xx} through Γ_{zz} inside and near a test prism set as a unit cube occupying the domain, $0 \le x \le 1$, $0 \le y \le 1$ and $0 \le z \le 1$, with the vertical density profiles consisting of monomials of z for the maximum degree, $N = 0$, 1, ..., 20. All the computer programs are written in Fortran 90, compiled by the Intel Visual Fortran Composer XE2011 update 8, that is, the so-called *ifort*12.1, with the compiler flags to enable the maximum optimization as

```
/O3 /Qparallel /Qpar-threshold:10 /Qvec-threshold:10
/Qopt-prefetch=3 /assume:buffered_io /Qipo /Qopt-matmul
/check:bounds /libs:static /threads /c
```

and executed at a consumer PC with the Intel Core i7-4600U running at 2.10 GHz clock. Fig. 3 illustrates the averaged CPU times in the unit of μs as a function of N for three cases: (i) the computation of V only, (ii) the computation of V, g_x, g_y and g_z simultaneously and (iii) the computation of the full set of V, g_x through g_z and Γ_{xx} through Γ_{zz}. We experimentally learn that the averaged CPU time for one execution of the elementary functions such as the logarithm or the arc tangent functions is 24 ns if employing the machine codes provided by the standard Intel mathematical function library. Since these functions are called $(3 + 3) \times 8 = 48$ times in a naive implementation of the homogeneous prism potential computation, we judge that the measured CPU time of around 1 μs when $N = 0$ is not so large.

On the other hand, the figure clearly indicates that the averaged CPU time increases slowly when N increases. This is because the new formulation utilizes the recursive computation such that the number of the transcendental function calls is independent on N. Rather, the observed slow increase of the CPU time is due to the increase of the number of recursions where only the arithmetic operations are needed. Also, the total CPU time increases only slightly when the number of the gravitational quantities to be computed increases from 1 when only V is computed, to 4 when g_x through g_z are additionally required, and to 10 when the full set of V, g_x, g_y, g_z and Γ_{xx} through Γ_{zz} are obtained. This is thanks to the simplicity of the derivative formulae of U_n which require no time-consuming operation additionally.

Finally, lest us compare the CPU time of the new method with that of the existing method (Zhang & Jiang 2017). Fig. 4 presents the CPU times of these two methods to compute g_z as a function of N when $0 \le N \le 40$. The figure shows the results in a log–log manner with respect to $N + 1$. Obviously, both the curves exhibit power-law-like growth. The broken lines indicate the piecewise power-law function models fitted to the measurements as

$$\text{CPU Time}_{\text{Zhang and Jiang (2017)}}/\mu\text{s} = \begin{cases} 5.62 \times (N+1)^{1.75}, & (0 \le N \le 14), \\ 0.0537 \times (N+1)^{3.50}, & (15 \le N \le 40), \end{cases} \tag{48}$$

$$\text{CPU Time}_{\text{new}}/\mu\text{s} = \begin{cases} 1.17 \times (N+1)^{0.25}, & (0 \le N \le 10), \\ 0.200 \times (N+1)^{1.00}, & (11 \le N \le 40). \end{cases} \tag{49}$$

Evidently, not only the initial magnitude but also the power index of the power-law manner of growth are significantly different between these two methods. In any case, it is clear that the new method is much faster than the existing method. Indeed, the acceleration factor increases from 30 to 2000 when N changes from 2 to 40. This achievement mainly owes to the adoption of a recursive formulation in the new method.

4 CONCLUSION

In order to describe the regional gravitational field in a more realistic manner, we considered a vertically inhomogeneous prism with the density profile being an arbitrary degree polynomial of the vertical coordinate. We developed a systematic method to compute the gravitational potential of the prism and its first- and second-order partial derivatives with respect to the rectangular coordinates. The method is purely analytic and utilizes the recurrence formulae to evaluate three groups of auxiliary functions, D_n, E_n and R_n, all of which turned out to be complicated elementary functions. Since the analytic expressions of the gravitational acceleration vector and the gravity gradient tensor are some sort of simplifications of that of the gravitational potential, the total computational labour to obtain all these three kind of quantities is merely the twice of that to compute the potential only despite the fact that the number of the gravitational quantities increases by a factor 10. As a result, the CPU time of the new formulation becomes fairly small and only slowly increases according as the maximum degree of the polynomial used in describing the density profile, say four times for the degree 9 polynomial. For example, even when required is the vertical gravity component only, it runs 30–2000 times faster than the existing formulation (Zhang & Jiang 2017) when the maximum degree of polynomial increases from 2 to 40.

Numerical experiments show that the computational errors of the gravitational field evaluated numerically by using the new formulation remain at the machine epsilon level if the evaluation point is inside or near the prism. However, they significantly increase in the far region. This unwelcome situation is caused by the round-off errors in the process of the triple difference. Of course, the effective region of the analytical procedure can be extended significantly if the quadruple precision computation is employed, say around 1000 times the prism size for the degree 9 polynomial density variation if the six digits precision is required. Nevertheless, this effective region significantly diminishes when higher degree polynomials are demanded such as in the case of an exponentially damped profile. Consequently, for the further improvement, we need a definitive solution to remove or suppress this type of accumulation of round-off errors as Holstein (2003) partially succeeded. Indeed, it is an issue worthwhile to be tackled in the future.

ACKNOWLEDGEMENTS

The author appreciates valuable suggestions and fruitful comments by Dr. Zhang and an anonymous referee to improve the quality of the article.

REFERENCES

Anderson, E.G., 1976. *The effect of topography on solutions of Stokes' problem, Unisurv S-14 Report, School of Surveying,* University of New South Wales, Kensington.

Benedek, J., Papp, G. & Kalmar, J., 2018. Generalization techniques to reduce the number of volume elements for terrain effect calculations in fully analytical gravitational modelling, *J. Geod.,* **92**(4), 361–381 .

Bessel, F.W., 1813. Auszug aus einen Schreien des Herrn Prof. Bessel, *Monatl. Corresp. Bef. Erd- und Himmels-Kunde,* **XXVII,** 80–85.

Binney, J. & Tremaine, S., 2008. *Galactic Dynamics,* 2nd edn, Princeton Univ. Press, Princeton.

Braitenberg, C., Wienecke, S. & Wang, Y., 2006. Basement structures from satellite-derived gravity field: South China Sea ridge, *J. geophys. Res.,* **111,** B05407.

Chai, Y. & Hinze, W.J., 1988. Gravity inversion of an interface above which the density contrast varies exponentially with depth, *Geophysics,* **53,** 837–845.

Chakravarthi, V., Raghuram, H.M. & Singh, S.B., 2002. 3-D forward gravity modeling of basement interfaces above which the density contrast varies continuously with depth, *Comp. Geosci.,* **28,** 53–57.

Chakravarthi, V., Raamamma, B. & Venkat Reddy, T., 2013. Gravity anomaly modelling o sedimentary basins by means o multiple structures and exponential density contrast-depth variations: a space domain approach, *J. Geol. Soc. India,* **82,** 561–569.

Chandrasekhar, S., 1969. *Ellipsoidal Figures of Equilibrium,* Yale Univ. Press, Dover, New York, (reprinted 1987).

Chandrasekhar, S., 1995. *Newton's Principia for the Common Reader,* Oxford Univ. Press, Oxford.

Chappell, A. & Kusznir, N., 2008. An algorithm to calculate the gravity anomaly of sedimentary basins with exponential density-depth relationships, *Geophys. Prosp.,* **56,** 249–258.

Conway, J.T., 2015. Analytical solutions from vector potentials for the gravitational field of a general polyhedron, *Celest. Mech. Dyn. Astron.,* **121,** 17–38.

Cordell, L., 1973. Gravity analysis using an exponential density-depth function–San Jacinto graben, California, *Geophysics,* **38,** 684–690.

de Pater, I. & Lissauer, J.J., 2010. *Planetary Sciences,* 2nd edn, Cambridge Univ. Press, London.

Durand, E., 1953. *Electrostatique et Magnetostatique,* Masson et Cie, Paris.

D'Urso, M.G., 2014. Analytical computation of gravity effects for polyhedral bodies, *J. Geod.,* **88,** 13–29.

D'Urso, M.G. & Trotta, S., 2017. Gravity anomaly of polyhedral bodies having a polynomial density contrast, *Surv. Geophys.,* **38,** 781–832.

Eshagh, M., 2009. Spherical harmonics expansion of the atmospheric gravitational potential based on exponential and power models of atmosphere, *Artif. Sat.,* **43,** 25–43.

Eshagh, M. & Sjöberg, L.E., 2009. Atmospheric effects on satellite gravity gradiometry data, *J. Geodyn.,* **47,** 9–19.

Fukushima, T., 2018. Accurate computation of gravitational field of a tesseroid, *J. Geod.*

Garcia-Abdeslem, J., 1992. Gravitational attraction of a rectangular prism with depth-dependent density, *Geophysics,* **57,** 470–473.

Garcia-Abdeslem, J., 2005. Gravitational attraction of a rectangular prism with density varying with depth following a cubic polynomial, *Geophysics,* **70,** J39–J42.
Granser, H., 1987. Three-dimensional interpretation of gravity data from sedimentary basins using an exponential density-depth function, *Geophys. Prosp.,* **35,** 1030–1041.
Heck, B. & Seitz, K., 2007. A comparison of the tesseroid, prism and point-mass approaches for mass reductions in gravity field modelling, *J. Geod.,* **81,** 121–136.
Heiskanen, W.A. & Moritz, H., 1967. *Physical Geodesy,* Freeman, San Francisco.
Holstein, H., 2003. Gravimagnetic anomaly formulas for polyhedra of spatially linear media, *Geophysics,* **68,** 157–167.
IEEE Comp. Soc., 2008. *IEEE Standard for Floating-Point Arithmetic (IEEE Std 754-2008)*. IEEE, New York.
Jiang, L., Zhang, J.-Z. & Feng, Z.-B., 2017a. A versatile solution for the gravity anomaly of 3D prism-meshed bodies with depth-dependent density contrast, *Geophysics,* **82,** G77–G86.
Jiang, L., Liu, J., Zhang, J.-Z. & Feng, Z.-B., 2017b. Analytic expressions for the gravity gradient tensor of 3D prisms with depth-dependent density, *Surv. Geophys.*
Karcol, R., 2011. Gravitational attraction and potential of spherical shell with radially dependent density, *Stud. Geophys. Geod.,* **55,** 21–34.
Kellogg, O.D., 1929. *Foundations of Potential Theory,* Springer, Berlin.
Laplace, P.S., 1799. *Traité de Mécanique Céleste,* Tome 1, Chez J. B. M. Duprat, Paris.
Lass, H., 1950. *Vector and Tensor Analysis,* McGraw-Hill, New York.
Li, X., 2001. Vertical resolution: gravity versus vertical gravity gradient, *Leading Edge,* **20,** 901–904.
MacMillan, W.D., 1930. *The Theory of the Potential,* McGraw-Hill, New York.
Mollweide, K.B., 1813. Auflösung einiger die Anziehing von Linien Flächen und Köpern betreffenden Aufgaben unter denen auch die in der Monatl. Corresp. Bd XXIV. S. 522. vorgelegte sich findet, *Monatl. Corresp. Bef. Erd- und Himmels-Kunde,* **XXVII,** 26–38.
Nagy, D., Papp, G. & Benedek, J., 2000. The gravitational potential and its derivatives for the prism, *J. Geod.,* **74,** 552–560.
Novak, P., 2000. Evaluation of gravity data for the Stokes-Helmert solution to the geodetic boundary-value problem, *Tech. Rep. Dept. Geod. Geom. Eng. Univ. New Brunswick,* **207**.
Rao, C.V., Raju, M.L. & Chakravarthi, V., 1995. Gravity modeling of an interface above which the density contrast decreases hyperbolically with depth, *J. appl. Geophys.,* **34,** 63–67.
Rao, D.B., 1985. Analysis of gravity anomalies over an inclined fault with quadratic density function, *Pure appl. Geophys.,* **123,** 250–260.
Rao, D.B., Prakash, M.J. & Babu, N.R., 1990. 3D and 2.5D modelling of gravity anomalies with variable density contrast, *Geophys. Prosp.,* **38,** 411–422.
Sjöberg, L.E., 1998. The atmospheric geoid and gravity corrections, *Boll. Geod. Sci. Aff.,* **4,** 421–435.
Sjöberg, L.E. & Bagherbandi, M., 2017. *Gravity Inversion and Integration,* Springer, Berlin.
Sjöberg, L.E. & Nahavandchi, H., 2000. The atmospheric geoid effects in Stokes formula, *Geophys. J. Int.,* **140,** 95–100.
Smith, B. & Sandwell, D., 2003. Accuracy and resolution of shuttle radar topography mission data, *Geophys. Res. Lett.,* **32,** L21S01.
Stacey, F.D. & Davis, P.M., 2008. *Physics of the Earth,* 4th edn, Cambridge Univ. Press, Cambridge.
Tachikawa, T., Hato, M., Kaku, M. & Iwasaki, A., 2011. Characteristics of ASTER GDEM version 2, in *Proc. IEEE Int'l Geosci. Remote Sensing Symp.,* Vol. **2011,** pp. 3657–3660, IEEE.
Tsoulis, D. & Petrovic, S., 2001. On the singularities of the gravity field of a homogeneous polyhedral body, *Geophysics,* **66,** 535–539.
Waldvogel, J., 1979. The Newtonian potential of uniform polyhedra, *Zeitschr. Angew. Math. Phys.,* **30,** 388–398.
Wild-Pfeiffer, F., 2008. A comparison of different mass elements for use in gravity gradiometry, *J. Geod.,* **82,** 637–653.
Wolfram, S., 2003. *The Mathematica Book,* 5th edn, Wolfram Research Inc./Cambridge Univ. Press, Cambridge.
Zhang, J.-Z. & Jiang, L., 2017. Analytical expressions for the gravitational vector field of a 3-D rectangular prism with density varying as an arbitrary-order polynomial function, *Geophys. J. Int.,* **210,** 1176–1190.

APPENDIX A: DERIVATION OF RECURSIVE PROCEDURE TO EVALUATE POTENTIAL FUNCTIONS

A1 Basic integral formulae

Let us derive the recursive procedure to compute the potential functions, U_n, given in the main text. First of all, we show some integral formulae:

$$\int^{X} \frac{\mathrm{d}X}{R} = \ln(X+R), \tag{A1}$$

$$\int^{Y} \ln(X+R)\mathrm{d}Y = Z\tan^{-1}\left(\frac{Y}{Z}\right) - Y - Z\tan^{-1}\left(\frac{XY}{ZR}\right) + X\ln(Y+R) + Y\ln(X+R), \tag{A2}$$

$$\int^{Z} Z\tan^{-1}\left(\frac{XY}{ZR}\right)\mathrm{d}Z = XY\ln(Z+R) - \left(\frac{X^2}{2}\right)\tan^{-1}\left(\frac{YZ}{XR}\right) - \left(\frac{Y^2}{2}\right)\tan^{-1}\left(\frac{XZ}{YR}\right) + \left(\frac{Z^2}{2}\right)\tan^{-1}\left(\frac{XY}{ZR}\right), \tag{A3}$$

where R is an abbreviation as

$$R \equiv \sqrt{X^2+Y^2+Z^2}. \tag{A4}$$

The correctness of all these integral formulae is confirmed by their direct partial differentiation.

A2 Line integral representation of U_n

By using the formulae shown in the previous subsection, we rewrite W_n as

$$\begin{aligned} W_n &= \int^Z \left[\int^Y \left(\int^X \frac{\mathrm{d}X}{R}\right)\mathrm{d}Y\right] Z^n \mathrm{d}Z\Big|_{X=X_1}^{X=X_2}\Big|_{Y=Y_1}^{Y=Y_2}\Big|_{Z=Z_1}^{Z=Z_2} \\ &= \int^Z \left[\int^Y \ln(X+R)\mathrm{d}Y\right] Z^n \mathrm{d}Z\Big|_{X=X_1}^{X=X_2}\Big|_{Y=Y_1}^{Y=Y_2}\Big|_{Z=Z_1}^{Z=Z_2} \\ &= \int^Z \left[Z^n\left\{Z\tan^{-1}\left(\frac{Y}{Z}\right) - Y\right\} - Z^{n+1}\tan^{-1}\left(\frac{XY}{ZR}\right)\right. \\ &\quad \left. + Z^n X\ln(Y+R) + Z^n Y\ln(X+R)\right]\mathrm{d}Z\Big|_{X=X_1}^{X=X_2}\Big|_{Y=Y_1}^{Y=Y_2}\Big|_{Z=Z_1}^{Z=Z_2}. \end{aligned} \tag{A5}$$

The first term of the last integrand, $Z^n\{Z\tan^{-1}(Y/Z) - Y\}$, is independent on X. Thus, its integral will disappear in the difference with respect to X. Therefore, we omit it before the integration. Let us call this operation 'reduction'. As a result, we arrive at the reduced line integral representation of U_n as

$$U_n = \left(\int^Z \left[-Z^{n+1}\tan^{-1}\left(\frac{XY}{ZR}\right) + XZ^n\ln(Y+R) + YZ^n\ln(X+R)\right]\mathrm{d}Z\right)^*, \tag{A6}$$

where the parentheses with an asterisk means the result after the reduction.

A3 Analytical expression of U_n

The derivatives of the second multiplier of each term of the last integrand in eq. (A6) are written as

$$\frac{\partial}{\partial Z}\left[\tan^{-1}\left(\frac{XY}{ZR}\right)\right] = -\left(\frac{1}{X^2+Z^2} + \frac{1}{Y^2+Z^2}\right)\frac{XY}{R}, \frac{\partial\ln(X+R)}{\partial Z} = \frac{Z}{(X+R)R}, \quad \frac{\partial\ln(Y+R)}{\partial Z} = \frac{Z}{(Y+R)R}. \tag{A7}$$

Using these, we rewrite U_n by the integration by part as

$$\begin{aligned} U_n &= \left(\int^Z \left[-\left\{\frac{\partial}{\partial Z}\left(\frac{Z^{n+2}}{n+2}\right)\right\}\tan^{-1}\left(\frac{XY}{ZR}\right)\right. \\ &\quad \left. + \left\{\frac{\partial}{\partial Z}\left(\frac{Z^{n+1}}{n+1}\right)\right\}\{X\ln(Y+R) + Y\ln(X+R)\}\right]\mathrm{d}Z\right)^* \\ &= \left[-\left(\frac{Z^{n+2}}{n+2}\right)\tan^{-1}\left(\frac{XY}{ZR}\right) + \left(\frac{Z^{n+1}}{n+1}\right)\{X\ln(Y+R) + Y\ln(X+R)\}\right]\Big|^Z \\ &\quad - \frac{X}{n+2}\left(\int^Z \frac{YZ^{n+2}\mathrm{d}Z}{(X^2+Z^2)R}\right)^* - \frac{X}{n+1}\left(\int^Z \frac{Z^{n+2}\mathrm{d}Z}{(Y+R)R}\right)^* \\ &\quad - \frac{Y}{n+2}\left(\int^Z \frac{XZ^{n+2}\mathrm{d}Z}{(Y^2+Z^2)R}\right)^* - \frac{Y}{n+1}\left(\int^Z \frac{Z^{n+2}\mathrm{d}Z}{(X+R)R}\right)^*. \end{aligned} \tag{A8}$$

Except the difference in their signs, the last two reduced integrals are the same with each other because

$$\begin{aligned} \left(\int^Z \frac{XZ^{n+2}\mathrm{d}Z}{(Y^2+Z^2)R}\right)^* + \left(\int^Z \frac{Z^{n+2}\mathrm{d}Z}{(X+R)R}\right)^* &= \left(\int^Z \frac{\left[X(X+R) + \left(Y^2+Z^2\right)\right]Z^{n+2}\mathrm{d}Z}{(Y^2+Z^2)(X+R)R}\right)^* \\ &= \left(\int^Z \frac{\left(R^2+XR\right)Z^{n+2}\mathrm{d}Z}{(Y^2+Z^2)(R^2+XR)}\right)^* = \left(\int^Z \frac{Z^{n+2}\mathrm{d}Z}{Y^2+Z^2}\right)^* = 0, \end{aligned} \tag{A9}$$

since the integrand of the last expression is independent on X. Similar equivalence is shown for the second last pair of the reduced integrals.

Based on these observations, let us introduce a pair of new reduced integrals, D_n and E_n, defined as

$$D_n \equiv \left(\int^Z \frac{Z^n\mathrm{d}Z}{(X+R)R}\right)^*, \quad E_n \equiv \left(\int^Z \frac{Z^n\mathrm{d}Z}{(Y+R)R}\right)^*. \tag{A10}$$

Then, by using these new integrals, we rewrite U_n as

$$U_n = -\left(\frac{Z^{n+2}}{n+2}\right)\tan^{-1}\left(\frac{XY}{ZR}\right) + \frac{Z^{n+1}}{n+1}\left[X\ln(Y+R) + Y\ln(X+R)\right] - \left(\frac{XE_{n+2} + YD_{n+2}}{(n+1)(n+2)}\right). \tag{A11}$$

This is the same as eq. (26) in the main text.

Note that $\varphi_j(x, z)$, the special function introduced in Zhang & Jiang (2017, eq. 18), is defined as

$$\varphi_j(X, Z) = \int^Z \frac{Z^{j+1}\mathrm{d}Z}{(X^2 + Z^2)\,R}. \tag{A12}$$

Consequently, apart from the reducible components, it is essentially the same as D_n and E_n as

$$D_n = -X\varphi_{n-1}(Y, Z), \quad E_n = -Y\varphi_{n-1}(X, Z). \tag{A13}$$

This is the same as eq. (35) in the main text.

A4 Recursive computation of D_n and E_n

Let us find the recurrence formulae to evaluate D_n and E_n for positive integer indices, n. First of all, their analytical expressions for $n = 1$ and 2 are explicitly obtained by their direct integration as

$$\begin{aligned} D_1 &= \ln(X + R), \quad D_2 = Y\tan^{-1}\left(\frac{ZX}{YR}\right) - X\ln(Z + R), \\ E_1 &= \ln(Y + R), \quad E_2 = X\tan^{-1}\left(\frac{YZ}{XR}\right) - Y\ln(Z + R), \end{aligned} \tag{A14}$$

where we omitted the reducible contributions. The correctness of these formulae is confirmed by their direct partial differentiation with respect to Z as

$$\frac{\partial D_n}{\partial Z} = \frac{Z^n}{(X + R)R}, \quad \frac{\partial E_n}{\partial Z} = \frac{Z^n}{(Y + R)R}. \tag{A15}$$

Next, noting the identity relation,

$$1 - \frac{X^2 + Z^2}{(Y + R)R} = \frac{(Y + R)R - X^2 - Z^2}{(Y + R)R} = \frac{YR + R^2 - X^2 - Z^2}{(Y + R)R} = \frac{YR + Y^2}{(Y + R)R} = \frac{Y(Y + R)}{(Y + R)R} = \frac{Y}{R}, \tag{A16}$$

we rewrite a linear combination of E_n as

$$X^2E_{n-2} + E_n = \left(\int^Z \frac{Z^{n-2}\left(X^2 + Z^2\right)}{(Y + R)R}\mathrm{d}Z\right)^* = \left(\int^Z \left[Z^{n-2} - \frac{Z^{n-2}Y}{R}\right]\mathrm{d}Z\right)^* = -YR_{n-2}, \tag{A17}$$

where R_n is another reduced integral defined as

$$R_n \equiv \left(\int^Z \frac{Z^n\mathrm{d}Z}{R}\right)^*. \tag{A18}$$

In the above rewriting, we used the identity relation

$$\left(\int^Z Z^{n-2}\mathrm{d}Z\right)^* = 0, \tag{A19}$$

since the integral is independent on X and Y. A similar relation holds on D_n as

$$Y^2D_{n-2} + D_n = -XR_{n-2}. \tag{A20}$$

Thus, we translate these results into the recurrence relations of D_n and E_n as

$$D_n = -Y^2D_{n-2} - XR_{n-2}, \quad E_n = -X^2E_{n-2} - YR_{n-2}, \tag{A21}$$

where their initial values when $n = 1$ and 2 are already given in eq. (A14). Thus, the problem is reduced to the computation of R_n.

A5 Recursive computation of R_n

Let us consider the computation of R_n when n is a positive integer. Recalling a differential formula

$$\frac{\partial R}{\partial Z} = \frac{Z}{R}, \tag{A22}$$

we rewrite R_n by the integration by part as

$$\begin{aligned} R_n &= \left(\int^Z Z^{n-1}\left[\frac{Z}{R}\right]\mathrm{d}Z\right)^* = \left(\int^Z Z^{n-1}\left[\frac{\partial R}{\partial Z}\right]\mathrm{d}Z\right)^* = Z^{n-1}R\Big|^Z - \left(\int^Z (n-1)Z^{n-2}R\mathrm{d}Z\right)^* \\ &= Z^{n-1}R - (n-1)\left(\int^Z \frac{R^2Z^{n-2}}{R}\mathrm{d}Z\right)^* \\ &= Z^{n-1}R - (n-1)S\left(\int^Z \frac{Z^{n-2}\mathrm{d}Z}{R}\right)^* - (n-1)\left(\int^Z \frac{Z^n\mathrm{d}Z}{R}\right)^* \\ &= Z^{n-1}R - (n-1)SR_{n-2} - (n-1)R_n, \end{aligned} \tag{A23}$$

where S is the square sum of the horizontal coordinates defined as

$$S \equiv X^2 + Y^2, \tag{A24}$$

and we used the identity relation,

$$R^2 = S + Z^2. \tag{A25}$$

In any case, eq. (A23) is further rewritten into a recurrence relation of R_n as

$$nR_n = Z^{n-1}R - (n-1)SR_{n-2}. \tag{A26}$$

On the other hand, the special values when $n = 0$ and 1 are obtained by the direct analytical integration as

$$R_0 = \left(\int^Z \frac{\mathrm{d}Z}{R}\right)^* = \ln(Z+R), \quad R_1 = \left(\int^Z \frac{Z\mathrm{d}Z}{R}\right)^* = R. \tag{A27}$$

Thus, utilizing the recurrence formula, we obtain the case $n = 2$ as

$$R_2 = \frac{ZR - SR_0}{2} = \frac{ZR - S\ln(Z+R)}{2}. \tag{A28}$$

The correctness of this procedure is confirmed by the differential form of the defining integral with respect to Z as

$$\frac{\partial R_n}{\partial Z} = \frac{Z^n}{R}. \tag{A29}$$

This has closed the recursive procedure to evaluate R_n.

A6 Recursive computation of U_n

Now that a recurrence relation of R_n is known, the recursive formulations to evaluate D_n and E_n are closed, and therefore the analytical procedure to evaluate U_n is completed. By introducing the abbreviations

$$\begin{aligned} &A \equiv \tan^{-1}\left(\frac{YZ}{XR}\right), \quad B \equiv \tan^{-1}\left(\frac{ZX}{YR}\right), \quad C \equiv \tan^{-1}\left(\frac{XY}{ZR}\right), \\ &D \equiv \ln(X+R), \quad E \equiv \ln(Y+R), \quad F \equiv \ln(Z+R), \end{aligned} \tag{A30}$$

we summarize the recurrence formulae compactly as

$$\begin{aligned} &R_1 = R, \quad R_2 = \frac{ZR - SF}{2}. \quad R_n = \frac{Z^{n-1}R - (n-1)SR_{n-2}}{n}, \\ &D_1 = D, \quad D_2 = YB - XF, \quad D_n = -Y^2D_{n-2} - XR_{n-2}, \\ &E_1 = E, \quad E_2 = XA - YF, \quad E_n = -X^2E_{n-2} - YR_{n-2}, \\ &U_n = -\frac{Z^{n+2}C}{n+2} + \frac{Z^{n+1}(YD+XE)}{n+1} - \frac{YD_{n+2} + XE_{n+2}}{(n+1)(n+2)}. \end{aligned} \tag{A31}$$

These expressions are the same as those given in the main text.

APPENDIX B: DERIVATION OF ANALYTICAL EXPRESSION OF PARTIAL DERIVATIVES OF POTENTIAL FUNCTIONS

B1 Z-derivatives

Let us derive the derivative expressions of U_n. We begin with the Z-derivatives, namely U_{nZ}, U_{nXZ}, U_{nYZ} and U_{nZZ}. The line integral expression of U_n, eq. (A6), is of the form of an indefinite integral with respect to Z. Therefore, it immediately results the reduced expression of its partial

derivative with respect to Z as

$$U_{nZ} \equiv \left(\frac{\partial U_n}{\partial Z}\right)^* = -Z^{n+1}\tan^{-1}\left(\frac{XY}{ZR}\right) + XZ^n\ln(Y+R) + YZ^n\ln(X+R). \tag{B1}$$

Also, by using the integral formula, eq. (A2), in the differential form, we obtain the Y-derivative of U_{nZ} as

$$U_{nYZ} \equiv \left(\frac{\partial^2 U_n}{\partial Y \partial Z}\right)^* = \left(\frac{\partial}{\partial Y}\left(\frac{\partial U_n}{\partial Z}\right)^*\right)^* = Z^n\ln(X+R). \tag{B2}$$

Since U_{nZ} is symmetric with respect to X and Y, we similarly obtain the X-derivative of U_{nZ} as

$$U_{nXZ} \equiv \left(\frac{\partial^2 U_n}{\partial X \partial Z}\right)^* = Z^n\ln(Y+R). \tag{B3}$$

Finally, we focus on U_{nZZ}. First of all, U_{0ZZ} is evaluated by the direct partial differentiation of U_{0Z} with respect to Z as

$$U_{0ZZ} = \left(\frac{\partial U_{0Z}}{\partial Z}\right)^* = \left(\frac{XZ}{X^2+Z^2} + \frac{YZ}{Y^2+Z^2} - \tan^{-1}\left(\frac{XY}{ZR}\right)\right)^* = -\tan^{-1}\left(\frac{XY}{ZR}\right), \tag{B4}$$

where the first two terms in the last parentheses with an asterisk are omitted because they are independent on either Y or X, and therefore will disappear in the triple difference. Next, we regard U_{nZ} as a product of U_{0Z} and Z^n as

$$U_{nZ} = Z^n\left[-Z\tan^{-1}\left(\frac{XY}{ZR}\right) + X\ln(Y+R) + Y\ln(X+R)\right] = Z^n U_{0Z}. \tag{B5}$$

Thus, its reduced derivative with respect to Z is computed as

$$\begin{aligned} U_{nZZ} &\equiv \left(\frac{\partial U_{nZ}}{\partial Z}\right)^* = Z^n U_{0ZZ} + nZ^{n-1}U_{0Z} \\ &= Z^n\left[-\tan^{-1}\left(\frac{XY}{ZR}\right)\right] + nZ^{n-1}\left[-Z\tan^{-1}\left(\frac{XY}{ZR}\right) + X\ln(Y+R) + Y\ln(X+R)\right] \\ &= -(n+1)Z^n\tan^{-1}\left(\frac{XY}{ZR}\right) + nZ^{n-1}\left[X\ln(Y+R) + Y\ln(X+R)\right]. \end{aligned} \tag{B6}$$

B2 Other derivatives

Let us move on to the other derivatives, namely U_{nX}, U_{nY}, U_{nXX}, U_{nXY} and U_{nYY}. For this purpose, we consider another line integral expression of U_n by exchanging the order of three integrations as

$$U_n = \left(\int^X\left[\int^Y\left(\int^Z \frac{Z^n \mathrm{d}Z}{R}\right)\mathrm{d}Y\right]\mathrm{d}X\right)^* = \left(\int^X\left[\int^Y R_n \mathrm{d}Y\right]\mathrm{d}X\right)^*, \tag{B7}$$

where we used the definition of R_n, eq. (A18). This integral expression of U_n immediately leads to the expression of U_{nXY} as

$$U_{nXY} = \left(\frac{\partial^2 U_n}{\partial X \partial Y}\right)^* = R_n. \tag{B8}$$

Next, in order to obtain the expression of U_{nX}, we select yet another line integral expression of U_n as

$$U_n = \left(\int^X\left[\int^Z\left(\int^Y \frac{\mathrm{d}Y}{R}\right)Z^n\mathrm{d}Z\right]\mathrm{d}X\right)^* = \left(\int^X\left[\int^Z Z^n\ln(Y+R)\mathrm{d}Z\right]\mathrm{d}X\right)^*, \tag{B9}$$

where we used the integral formula, eq. (A1). This integral expression of U_n results a line integral expression of U_{nX} as

$$U_{nX} = \left(\frac{\partial U_n}{\partial X}\right)^* = \left(\int^Z Z^n\ln(Y+R)\mathrm{d}Z\right)^*. \tag{B10}$$

This integral has already appeared as the second term in the first line integral expression of U_n, eq. (A6). Repeating the rewriting procedure by using the integration by part, we obtain its rewriting as

$$\begin{aligned} U_{nX} &= \left(\int^Z\left\{\frac{\partial}{\partial Z}\left(\frac{Z^{n+1}}{n+1}\right)\right\}\ln(Y+R)\mathrm{d}Z\right)^* = \left[\left(\frac{Z^{n+1}}{n+1}\right)\ln(Y+R)\right]\Bigg|^Z - \frac{1}{n+1}\left(\int^Z \frac{Z^{n+2}\mathrm{d}Z}{(Y+R)R}\right)^* \\ &= \left(\frac{Z^{n+1}}{n+1}\right)\ln(Y+R) - \frac{E_{n+2}(X,Y,Z)}{n+1}. \end{aligned} \tag{B11}$$

Third, noting the differential formula written as

$$\frac{\partial}{\partial X}\left[\ln(Y+R)\right] = \frac{X}{(Y+R)R}, \tag{B12}$$

we obtain an expression of U_{nXX} by partially differentiating the integral expression of U_{nX}, eq. (B10), as

$$U_{nXX} = \left(\frac{\partial U_{nX}}{\partial X}\right)^* = \left(\int^Z Z^n \left[\frac{\partial}{\partial X}\{\ln(Y+R)\}\right] \mathrm{d}Z\right)^* = \left(\int^Z \frac{XZ^n \mathrm{d}Z}{(Y+R)R}\right)^* = XE_n, \tag{B13}$$

where we used the integral definition of E_n given in eq. (A10). Finally, thanks to the symmetry of U_n with respect to X and Y, we obtain U_{nY} and U_{nYY} from U_{nX} and U_{nXX} by interchanging X and E_n with Y and D_n as

$$U_{nY} = \left(\frac{Z^{n+1}}{n+1}\right)\ln(X+R) - \frac{D_{n+2}}{n+1}, \quad U_{nYY} = YD_n. \tag{B14}$$